High Power Laser Science and Engineering, (2021), Vol. 9, e20, 7 pages.
doi:10.1017/hpl.2021.13

HIGH POWER LASER SCIENCE AND ENGINEERING

RESEARCH ARTICLE

Effective suppression of mode distortion induced by stimulated Raman scattering in high-power fiber amplifiers

Wei Gao[1,2,3], Wenhui Fan[1,3,5], Pei Ju[1,3], Gang Li[1,3], Yanpeng Zhang[2], Aifeng He[4], Qi Gao[1,3], and Zhe Li[1,3]

[1] *State Key Laboratory of Transient Optics and Photonics, Xi'an Institute of Optics and Precision Mechanics, Chinese Academy of Sciences, Xi'an 710119, China*

[2] *Key Laboratory for Physical Electronics and Devices of the Ministry of Education & Shaanxi Key Laboratory of Information Photonic Technique, Xi'an Jiaotong University, Xi'an 710049, China*

[3] *University of Chinese Academy of Sciences, Beijing 100049, China*

[4] *Key Laboratory on Applied Physics and Chemistry, Shaanxi Applied Physics and Chemistry Research Institute, Xi'an 710061, China*

[5] *Collaborative Innovation Center of Extreme Optics, Shanxi University, Taiyuan 030006, China*

(Received 23 November 2020; revised 27 February 2021; accepted 4 March 2021)

Abstract

Mode distortion induced by stimulated Raman scattering (SRS) has become a new obstacle for the further development of high-power fiber lasers with high beam quality. Here, an approach for effective suppression of the SRS-induced mode distortion in high-power fiber amplifiers has been demonstrated experimentally by adjusting the seed power (output power of seed source) and forward feedback coefficient of the rear port in the seed source. It is shown that the threshold power of the SRS-induced mode distortion can be increased significantly by reducing the seed power or the forward feedback coefficient. Moreover, it has also been found that the threshold power is extremely sensitive to the forward feedback power value from the rear port. The influence of the seed power on the threshold power can be attributed to the fact that the seed power plays an important role in the effective length of the gain fiber in the amplifier. The influence of the forward feedback coefficient on the threshold power can be attributed to the enhanced SRS configuration because the end surface of the rear port together with the fiber in the amplifier constitutes a half-opening cavity. This suppression approach will be very helpful to further develop the high-power fiber amplifiers with high beam quality.

Keywords: high-power fiber amplifiers; mode distortion; stimulated Raman scattering; suppression

1. Introduction

High-power fiber lasers have found a wide variety of applications in industry, science, and defense owing to high conversion efficiency, robustness, easy thermal management, and especially excellent beam quality[1–3]. The large-mode-area (LMA) double-cladding gain fibers and high-brightness semiconductor laser diodes (LDs) lead to an exponential evolution on the output power of fiber lasers in the past two decades[4]. However, the evolution is suffering from a sudden halt owing to mode degradation phenomena[5,6].

Initially, the mode degradation phenomenon observed experimentally is actually thermally-induced transverse mode instability (TMI)[7], which is mainly caused by the quantum-defect effect in the process of stimulated radiation and the photodarkening effect[8–10]. Tao *et al*. studied systematically the influence of a series of parameters of fiber lasers on the thermally-induced TMI[11–13], and established a comprehensive theoretical model[14]. Gao *et al*. explained the sudden-change mechanism of the thermally-induced TMI from the perspective of non-equilibrium phase transition[15]. Since the TMI was discovered, it has become a big challenge

Correspondence to: W. Fan, Xi'an Institute of Optics and Precision Mechanics, Chinese Academy of Sciences, No. 17 Xinxi Road, Xi'an 710119, China; Y. Zhang, Xi'an Jiaotong University, No. 28 Xianning West Road, Xi'an 710049, China. Email: fanwh@opt.ac.cn (W. Fan); ypzhang@xjtu.edu.cn (Y. Zhang)

to further enhance the output power of fiber lasers with high beam quality[1,5]. For this reason, a lot of approaches to suppress thermally-induced TMI have been proposed, such as optimizing the size and coil diameter of gain fibers, reducing the wavelength difference between the pump and signal light, and modulating pump power[16–26].

Shortly afterwards, a type of mode degradation phenomenon named the low-threshold TMI was also observed in few-mode fibers with high Yb doping concentration under the low pump power (few watts)[27,28]. The low-threshold TMI was also often considered together with the thermally-induced TMI in the study of mode instability[14,27]. The low-threshold TMI originates from the spatial hole burning effect caused by the inter-mode interference, which results in the long-period refractive index gratings (owing to different polarizability of the excited and unexcited Yb ions)[27]. Antipov *et al*. investigated the influence of several parameters of fiber lasers on the low-threshold TMI, and found that the low-threshold TMI can be suppressed dramatically by reducing the backward reflection from the output end surface[28–30].

Very recently, a new type of mode degradation phenomenon named mode distortion induced by stimulated Raman scattering (SRS) was proposed[31,32], but mode distortion and the SRS effect were considered as independent phenomena previously. The SRS-induced mode distortion occurs suddenly and the beam quality deteriorates at the same time once the output power of fiber laser exceeds a certain value (several hundred to several thousand watts), which exhibits obvious threshold behaviors[33]. The key characteristic of SRS-induced mode distortion was reported as follows: when SRS emerges, the SRS-induced mode distortion appears immediately, and when the SRS effect is suppressed, the SRS-induced mode distortion disappears immediately[31,34]. In addition, the SRS-induced mode distortion could cause time-domain fluctuations in the output power, and the fluctuation frequency is just several hertz[35].

Unfortunately, SRS-induced mode distortion has also become a major limitation for further developing high-power fiber lasers with high beam quality. Therefore, it is very important to develop effective suppression strategies on SRS-induced mode distortion. In fiber oscillators, Ye *et al*. proposed that SRS-induced mode distortion can be greatly suppressed by eliminating the external feedback[34]. In fiber amplifiers, Hejaz *et al*. also found that SRS-induced mode distortion can be suppressed by adjusting gain fiber length[31]. However, the approach for suppressing SRS-induced mode distortion in fiber amplifiers by adjusting seed power or forward feedback coefficient has not been reported previously. In summary, effective suppression strategies are still very scarce compared with the suppression strategies for thermally-induced TMI.

In this paper, we propose and demonstrate an approach to suppress SRS-induced mode distortion in high-power fiber amplifiers by adjusting the seed power (output power of seed source) and forward feedback coefficient of the rear port in the seed source. It is shown that the SRS-induced mode distortion can be suppressed significantly by reducing the seed power or forward feedback coefficient. Moreover, it is noteworthy that the SRS-induced mode distortion is extremely sensitive to the forward feedback power value from the rear port. The mechanism of the SRS-induced mode distortion has been discussed in detail, and the mechanism of the seed power and forward feedback coefficient on the threshold power of the SRS-induced mode distortion has also been analyzed. This suppression approach will be very helpful to further develop the high-power fiber amplifiers with high beam quality.

2. Experimental setup

The experimental setup used to investigate the approach for suppressing SRS-induced mode distortion is illustrated schematically in Figure 1. The high-power fiber laser contained a seed source and a power amplifier. A pair of 10/125 single-mode (SM) fiber Bragg gratings (FBGs) was employed as the high-reflectivity (HR) cavity mirror and output coupler (OC). The central wavelength of the FBGs was 1080 nm, and the reflectivity of the FBGs was 99% for HR and 10% for OC, respectively. In order to obtain high-power output, the seed source required a large cavity mode volume. Therefore, a 46-m-long multimode (MM) Yb-doped double-cladding fiber (LMA-YDF-20/400) was used as the gain medium. The core diameter of the gain fiber was 20 μm (numerical aperture (NA) = 0.065), the inner cladding diameter was 400 μm (NA = 0.46), and its absorption coefficient was 0.42 dB/m at 915 nm. This 'SM/MM/SM' cavity structure can be used to obtain an ideal SM high-power seed source with the beam quality factor (M^2) close to one. The Yb-doped fiber was pumped by 915 nm LDs and two $(6+1)\times 1$ combiners were employed in the bi-directional pumping configuration. The two cladding power strippers (CPSs) inside the cavity were utilized to dump out the residual pump light and a small amount of high-order mode (HOM) scattering light due to the SM/MM splice. The rear port of the seed source was generally cleaved at 0°, so 4% of the rear port power from facet reflection could be re-injected into the laser system. The seed laser was launched into a 34-m-long Yb-doped double-cladding fiber (LMA-YDF-20/400) by a $(6+1)\times 1$ combiner in a forward-pumped amplifier. The Yb-doped fiber pumped by 915 nm LDs was coiled with a 13 cm diameter. The residual pump light of the amplifier was dumped out by using a CPS. Moreover, a quartz block holder (QBH, Optoskand) was employed to output the high-power laser beam and suppress the backward light from the output port.

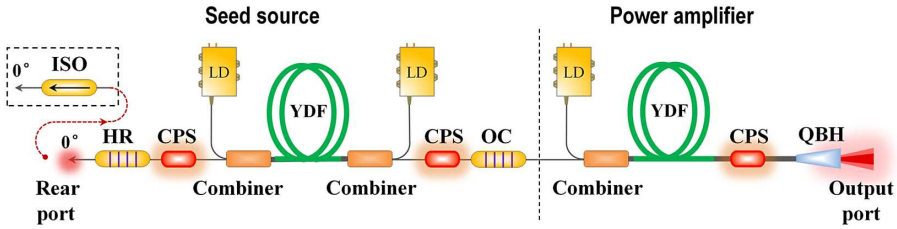

Figure 1. Schematic of the experimental setup. CPS, cladding power stripper; ISO, fiber isolator; LD, laser diode; QBH, quartz block holder; YDF, Yb-doped double-cladding fiber.

3. Experimental results

The seed power and the backward power (at the rear port) under different pump powers used in the seed source are shown in Figure 2(a). The measured seed power and backward power are shown by black and blue spheres, respectively, whereas the fitted seed power and backward power are represented by red and green lines, respectively. It can be seen that the seed power is up to 360 W when the injected pump power of seed source is 743 W. By linear fitting, the output slope efficiency of the seed source can be calculated as 49%. The low output slope efficiency of the seed source can be attributed to the large cavity loss due to the SM/MM splice. The backward power increases smoothly as the pump power of seed source increases.

When the seed laser with output power of 260 W was launched into the amplifier, the total output power (at the output port) and backward power (at the rear port) vary with different pump powers of the amplifier, as shown in Figure 2(b). By linear fitting, the output slope efficiency of the amplifier can be calculated as 66%. The low slope efficiency of the amplifier can be mainly attributed to the reabsorption effect of the unpumped part of the gain fiber in the amplifier. Note that the backward power is almost constant as the pump power of the amplifier increases, but it abruptly increases around 3.76 W once the pump power reaches 789 W (the total output power reaches 774 W). The abrupt point is marked with an orange dashed line in Figure 2(b), and the far-field beam profiles (together with the beam quality) near this abrupt point were recorded by the M^2 factor measuring instrument (PRIMES-HP-LQM), as shown in Figure 3. When the total output power is 695 W, the far-field beam profile follows an approximately Gaussian distribution and the M^2 factor is measured as 1.1, which is close to the ideal Gaussian beam. However, when the total output power is 774 W, the far-field beam profile is degraded, and the far-field profile area is increased because the generation of HOMs leads to the increased far-field divergence angle. At this time, it is impossible to measure the M^2 factor in validity, indicating a mode distortion occurring in the amplifier. When the total output power is reduced to 695 W again, the M^2 factor also returns to 1.1, and the backward power also drops back to its previous value (3.55 W).

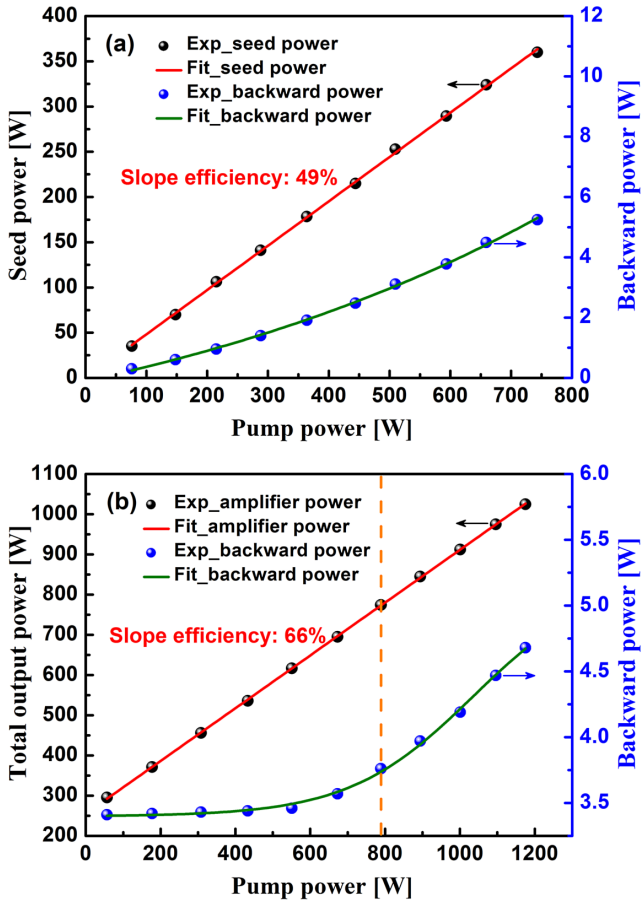

Figure 2. (a) Seed powers and backward powers under different pump powers. (b) Total output powers and backward powers under different pump powers at the seed power of 260 W.

Therefore, the abrupt increase of the backward power can be a signal of the mode distortion in the amplifier.

In order to identify the mode distortion, the forward spectra (at the output port) and backward spectra (at the rear port) near the abrupt point were measured, as shown in Figure 4. When the total output power is 695 W (before the abrupt point), there is almost no SRS component observed both in the forward and backward spectra. However, once the pump power exceeds the abrupt point, the SRS components both in the forward and backward spectra appear simultaneously. As can be seen in Figures 3 and 4, the SRS and the mode

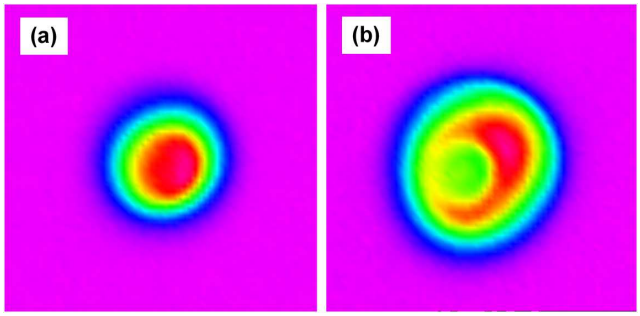

Figure 3. (a) The far-field beam profile before this abrupt point (695 W). (b) The far-field beam profile after this abrupt point (774 W).

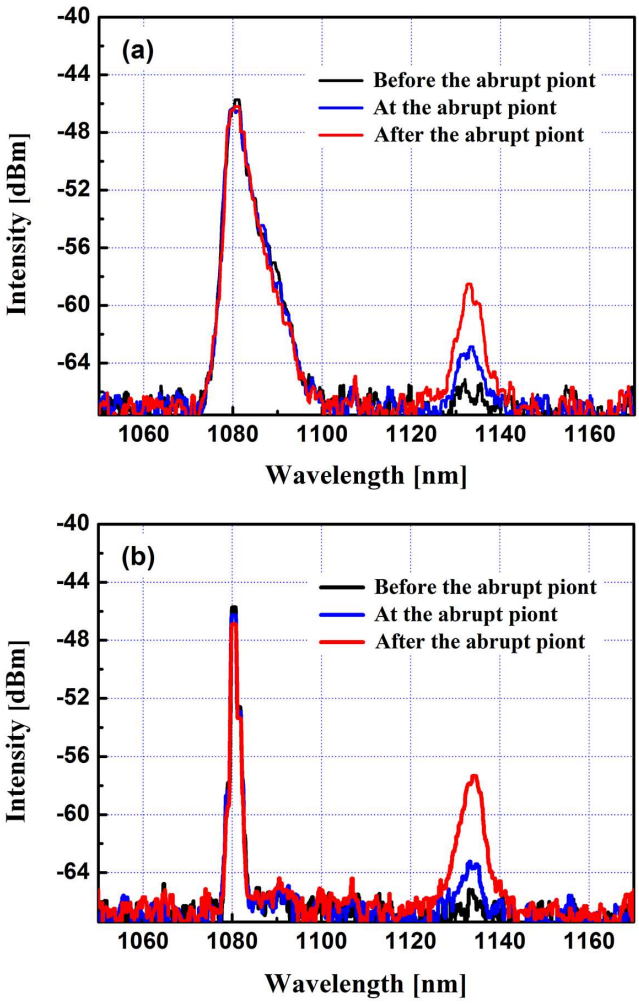

Figure 4. (a) Forward spectra near the abrupt point (at the output port). (b) Backward spectra near the abrupt point (at the rear port).

distortion appear almost simultaneously, strongly indicating the SRS-induced mode distortion occurring. The total output power (774 W) could be defined as the threshold power of the SRS-induced mode distortion. Moreover, it can be found in Figures 2(b) and 4(b) that the abrupt increase of the backward power can be attributed to the backward SRS.

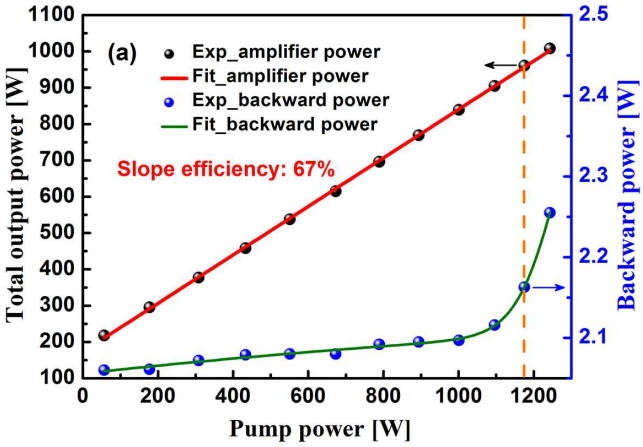

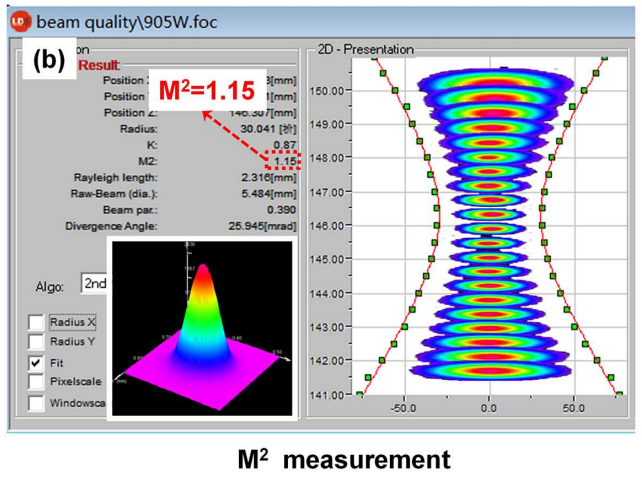

Figure 5. (a) The total output powers and backward powers under different pump powers at the seed power of 181 W. (b) Beam quality at the total output power of 905 W (before the abrupt point) at the seed power of 181 W.

In order to explore the influence of seed power on the threshold power of SRS-induced mode distortion, the seed power was reduced from 260 to 181 W. Figure 5(a) shows that the total output power and backward power vary with different pump powers of the amplifier when the seed power is fixed at 181 W. By linear fitting, the output slope efficiency of the amplifier is calculated as 67%, which is slightly higher than that at the seed power of 260 W. It is noteworthy that the backward power first slowly increases with the pump power increasing, and does not abruptly increase until the pump power is close to 1175 W. At this time, the total output power is 961 W. Figure 5(b) shows the beam quality taken at the total output power of 905 W (before the abrupt point), which is close to the ideal Gaussian beam because the M^2 factor can be measured as 1.15. At this time, no SRS signal was found both in the forward and backward spectra. However, when the total output power is 961 W, the beam quality is also severely degraded and the SRS signals both in the forward and backward spectra were also generated at the same time. As can be seen from Figures 5(a) and 5(b), the threshold power of SRS-induced mode distortion is 961 W.

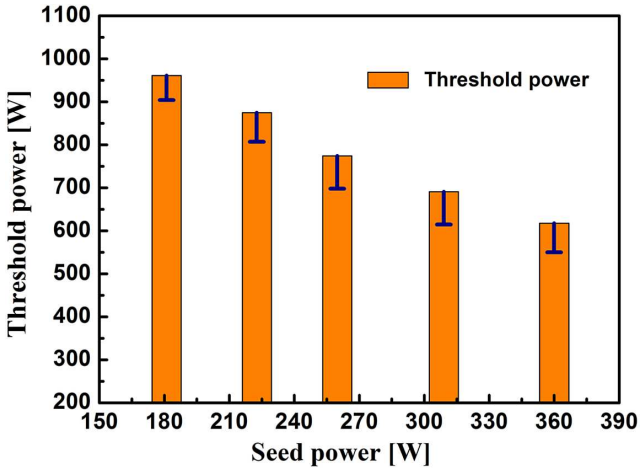

Figure 6. Threshold powers of the SRS-induced mode distortion under different seed powers.

Comparing Figure 5(a) with Figure 2(b), it can be found that the threshold power increases from 774 to 961 W (more than 24%) when the seed power decreases from 260 to 181 W. To further investigate the influence of the seed power on the threshold power of SRS-induced mode distortion, the threshold powers under different seed powers were measured, as shown in Figure 6. The inverted blue T-line in Figure 6 is the error bar. When the seed power was reduced to nearly half (181 W) from the maximum value (360 W), the threshold power rises from 618 to 961 W (more than 55%). This means that the threshold power increases significantly as the seed power decreases. In other words, the SRS-induced mode distortion can be suppressed significantly by reducing the seed power.

The dependence of the threshold power on the forward feedback coefficient of the rear port in the seed source was also investigated experimentally. In the experiment, the facet reflectivity of the rear port is 4%, so the forward feedback coefficient ($10\log(R)$) can be calculated as −14 dB, where R is the facet reflectivity of the rear port. As seen from Figure 3, the threshold power of the SRS-induced mode distortion is 774 W when the seed power is fixed at 260 W. In order to reduce the forward feedback coefficient, a broadband fiber isolator was reversely fused to the rear port, as shown in the dashed line box in Figure 1. The isolation and insertion losses of the fiber isolator are 25 and 0.8 dB, respectively. Note that the output port of the fiber isolator was also cleaved at 0°, and the forward feedback coefficient calculated was −39.8 dB. At this time, the total output powers and the backward powers under different pump powers were re-recorded at the seed power of 260 W, as shown in Figure 7(a). It is found that the output slope efficiency of the amplifier calculated is 67%, slightly higher than that at the forward feedback coefficient of −14 dB. Obviously, the total output power (1054 W) corresponding to the abrupt point in Figure 7(a) is significantly higher than that (774 W) shown in

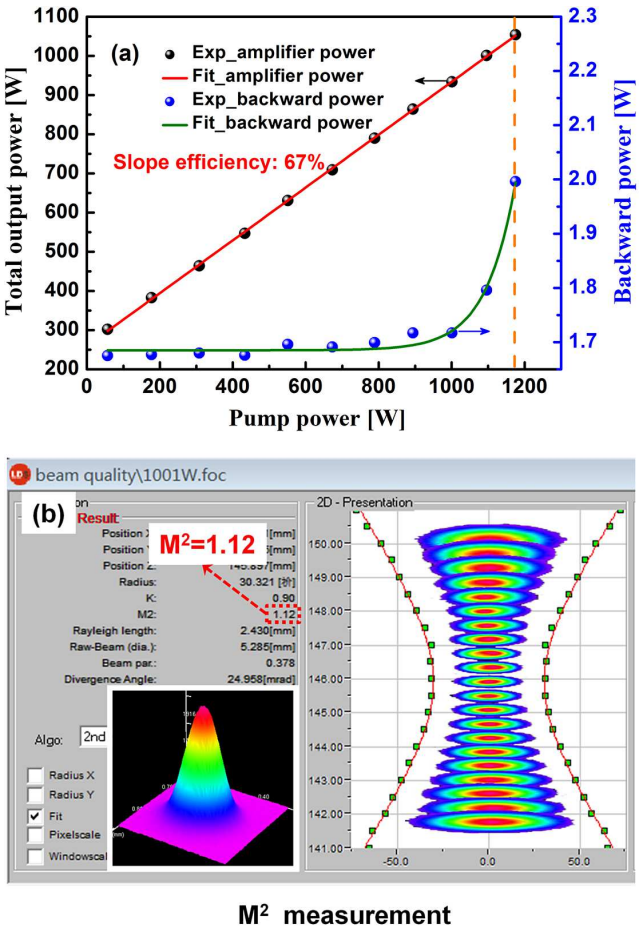

Figure 7. (a) Total output powers and backward powers under different pump powers at the seed power of 260 W. (b) Beam quality at the total output power of 1001 W (before the abrupt point) at the seed power of 260 W.

Figure 2(b). This means that the threshold power is increased by more than 36% when the forward feedback coefficient is reduced from −14 to −39.8 dB. Figure 7(b) shows the beam quality at the total output power of 1001 W (before the abrupt point), which is still close to the ideal Gaussian beam because the M^2 factor was measured as 1.12. When the total output power is 1054 W, the beam quality observed is also severely degraded, and the SRS signals were also generated both in the forward and backward spectra simultaneously.

To further reduce the forward feedback coefficient, a frosted silica rod was fused to the rear port instead of the broadband fiber isolator. The refractive index difference between two sides of the fusion point is 1.7×10^{-3}, because the refractive index of the silica rod is equal to that of the fiber cladding of the rear port. Therefore, the forward feedback coefficient can be calculated as −64.7 dB. The threshold power at the forward feedback coefficient of −64.7 dB was also measured. It is found that the beam quality is still close to the ideal Gaussian beam even when the total output power reaches the maximum output power,

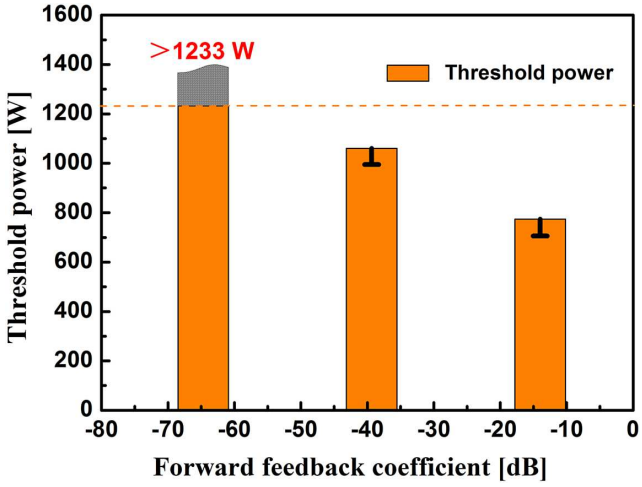

Figure 8. Threshold powers of the SRS-induced mode distortion under different forward feedback coefficients.

which was recorded as 1233 W and limited to the maximal power handling of the pump combiner. This indicates that the threshold power at the forward feedback coefficient of −64.7 dB can be more than 1233 W. Figure 8 shows that the threshold power varies with three forward feedback coefficients. It can be clearly seen that the threshold power increases significantly as the forward feedback coefficient decreases.

It is noteworthy that the SRS-induced mode distortion is extremely sensitive to the forward feedback power value. As long as there exists a bit of forward feedback power from the rear port, it will have a significant effect on the SRS-induced mode distortion. For example, if the backward power is 2 W, the forward feedback power values corresponding to above three forward feedback coefficients are 0.68 μW, 0.23 mW, and 80 mW, respectively. Compared with the total output power (∼1000 W), the feedback power value seems to be negligible, but it will affect the threshold power of the SRS-induced mode distortion significantly (see also Figure 8).

4. Discussion

According to Figures 3 and 4, it can be seen that the SRS-induced mode distortion occurred obviously, because the mode distortion and the SRS appeared almost simultaneously, which is also consistent with experimental results of the previous studies[31,32]. It can also been found that the SRS-induced mode distortion could originate directly from the nonlinear effects in MM fibers, rather than the thermally-induced TMI due to the quantum defect indirectly caused by the SRS process. The latter was used to explain the SRS-induced mode distortion in the previous study[31]. The reason is that at the beginning of the SRS effect, the heat production rate caused by the SRS process is too small to trigger the thermally-induced TMI. SRS-induced mode distortion may be due to the nonlinear mode coupling process[36,37] between modes of the signal laser and the SRS light. The likely explanation for SRS-induced mode distortion is that the generated SRS light immediately triggers the nonlinear mode coupling process, which leads to mode distortion. Therefore, the key strategy to suppress the SRS-induced mode distortion is to suppress the generation of the SRS light.

According to Figure 6, SRS-induced mode distortion can be suppressed significantly by reducing the seed power. The influence of the seed power on the threshold power can be attributed to the fact that the seed power significantly affects the effective length of the gain fiber in the amplifier. The effective length of a gain fiber is usually defined as $g^{-1}\left[\exp(gL)-1\right]$, where g and L are the gain coefficient and the length of the gain fiber, respectively[38]. When the total output power and the length of the gain fiber are fixed, the lower the seed power is, the higher the gain coefficient is, and the shorter effective length is, which leads to the higher threshold power of the SRS effect or the higher SRS-induced mode distortion.

From the analysis of Figures 7 and 8, SRS-induced mode distortion in the amplifier is extremely sensitive to the forward feedback power value and can also be suppressed significantly by reducing the forward feedback coefficient, which is similar to that in the oscillators[34]. The explanation for the influence of the forward feedback coefficient on the threshold power is more likely the enhanced SRS configuration because the end surface of the rear port in the seed source together with the fiber in the amplifier constitutes a half-opening cavity, which can also be regarded as a short-cavity random Raman laser with a half-opening cavity[39]. According to the threshold theory of random Raman lasers, when the cavity length is relatively short, even extremely weak forward feedback power can also provide very effective positive feedback for the SRS effect and play a critical role in reducing the threshold of random Raman lasers[40–42], and this is the reason why the SRS-induced mode distortion is extremely sensitive to the forward feedback power value. Thus, it can be seen that both of the above methods indirectly suppress SRS-induced mode distortion in fact by efficiently suppressing the SRS effect. As a consequence, we should adopt a low-power seed source and eliminate forward feedback as much as possible to obtain high-power fiber amplifiers with high beam quality.

5. Conclusion

In summary, an approach for effective suppression of the SRS-induced mode distortion in high-power fiber amplifiers has been demonstrated experimentally by adjusting seed power and forward feedback coefficient of the rear port in the seed source. The experimental results indicate that

SRS-induced mode distortion can be suppressed significantly by reducing the seed power. The influence of the seed power on the threshold power can be attributed to the fact that the seed power significantly affects the effective length of the gain fiber in the amplifier. Lower seed power leads to the shorter effective length and, as a result, the threshold power becomes higher. The experimental results also demonstrate that SRS-induced mode distortion can be suppressed significantly by reducing the forward feedback coefficient. Moreover, it was found that the threshold power was extremely sensitive to the forward feedback power value. Even extremely weak forward feedback power can provide very effective positive feedback for SRS-induced mode distortion or the SRS effect, and a half-opening cavity enhanced SRS configuration can be formed. All in all, the strong dependence of the threshold power of SRS-induced mode distortion in fiber amplifiers on the seed power, especially forward feedback coefficient, provides an effective approach to suppress the SRS-induced mode distortion, which is very beneficial for the development of high-power fiber amplifiers with high beam quality.

Acknowledgments

This work was supported by National Natural Science Foundation of China (Nos. 62005310 and 61675230), Equipment Pre-research Foundation of China (No. 61406190302), Key R&D Program of Shaanxi Province (No. 2018ZDXM-GY-060), and National Key R&D Program of China (No. 2017YFB1104400).

References

1. C. Jauregui, J. Limpert, and A. Tünnermann, Nat. Photonics **7**, 861 (2013).
2. J. Nilsson and D. N. Payne, Science **332**, 921 (2011).
3. Y. Wang, G. Chen, and J. Li, High Power Laser Sci. Eng. **6**, e40 (2018).
4. D. J. Richardson, J. Nilsson, and W. A. Clarkson, J. Opt. Soc. Am. B **27**, B63 (2010).
5. C. Stihler, C. Jauregui, A. Tünnermann, and J. Limpert, Light: Sci. Appl. **7**, 59 (2018).
6. C. Jauregui, C. Stihler, and J. Limpert, Adv. Opt. Photon. **12**, 429 (2020).
7. T. Eidam, C. Wirth, C. Jauregui, F. Stutzki, F. Jansen, H.-J. Otto, O. Schmidt, T. Schreiber, J. Limpert, and A. Tünnermann, Opt. Express **19**, 13218 (2011).
8. B. Ward, C. Robin, and I. Dajani, Opt. Express **20**, 11407 (2012).
9. Y. Fan, B. He, J. Zhou, J. Zheng, H. Liu, Y. Wei, J. Dong, and Q. Lou, Opt. Express **19**, 15162 (2011).
10. H.-J. Otto, N. Modsching, C. Jauregui, J. Limpert, and A. Tünnermann, Opt. Express **23**, 15265 (2015).
11. R. Tao, P. Ma, X. Wang, P. Zhou, and Z. Liu, IEEE J. Quantum Electron. **51**, 1600106 (2015).
12. R. Tao, P. Ma, X. Wang, P. Zhou, and Z. Liu, J. Opt. **19**, 065202 (2017).
13. Q. Chu, R. Tao, C. Li, H. Lin, Y. Wang, C. Guo, J. Wang, F. Jing, and C. Tang, Sci. Rep. **9**, 9396 (2019).
14. R. Tao, P. Ma, X. Wang, and P. Zhou, IEEE J. Sel. Top. Quant. **24**, 0903319 (2018).
15. W. Gao, B. Zhao, W. Fan, P. Ju, Y. Zhang, G. Li, Q. Gao, and Z. Li, Opt. Express **27**, 22393 (2019).
16. C. Jauregui, H.-J. Otto, F. Stutzki, F. Jansen, J. Limpert, and A. Tünnermann, Opt. Express **21**, 19375 (2013).
17. R. Tao, R. Su, P. Ma, X. Wang, and P. Zhou, Laser Phys. Lett. **14**, 025101 (2016).
18. K. Hansen and J. Lægsgaard, Opt. Express **22**, 11267 (2014).
19. H.-J. Otto, A. Klenke, C. Jauregui, F. Stutzki, J. Limpert, and A. Tünnermann, Opt. Lett. **39**, 2680 (2014).
20. C. Jauregui, H.-J. Otto, S. Breitkopf, J. Limpert, and A. Tünnermann, Opt. Express **24**, 7879 (2016).
21. R. Tao, P. Ma, X. Wang, P. Zhou, and Z. Liu, Photon. Res. **3**, 86 (2015).
22. H.-J. Otto, C. Jauregui, F. Stutzki, F. Jansen, J. Limpert, and A. Tünnermann, Opt. Express **21**, 17285 (2013).
23. C. Jauregui, C. Stihler, A. Tünnermann, and J. Limpert, Opt. Express **26**, 10691 (2018).
24. M. N. Zervas, APL Photonics **4**, 022802 (2019).
25. P. Ma, H. Xiao, D. Meng, W. Liu, R. Tao, J. Leng, Y. Ma, R. Su, P. Zhou, and Z. Liu, High Power Laser Sci. Eng. **6**, e57 (2018).
26. R. Cao, G. Chen, Y. Chen, Z. Zhang, X. Lin, B. Dai, L. Yang, and J. Li, Photon. Res. **8**, 288 (2020).
27. M. Kuznetsov, O. Vershinin, V. Tyrtyshnyy, and O. Antipov, Opt. Express **22**, 29714 (2014).
28. D. Alekseev, V. Tyrtyshnyy, M. Kuznetsov, and O. Antipov, IEEE J. Sel. Top. Quant. **24**, 5100608 (2018).
29. O. Antipov, M. Kuznetsov, V. Tyrtyshnyy, D. Alekseev, and O. Vershinin, Proc. SPIE **9728**, 97280A (2016).
30. O. Antipov, M. Kuznetsov, D. Alekseev, and V. Tyrtyshnyy, Opt. Express **24**, 14871 (2016).
31. K. Hejaz, M. Shayganmanesh, R. Rezaei-Nasirabad, A. Roohforouz, S. Azizi, A. Abedinajafi, and V. Vatani, Opt. Lett. **42**, 5274 (2017).
32. Z. Li, Z. Huang, X. Xiang, X. Liang, H. Lin, S. Xu, Z. Yang, J. Wang, and F. Jing, Photon. Res. **5**, 77 (2017).
33. R. Tao, H. Xiao, H. Zhang, J. Leng, X. Wang, P. Zhou, and X. Xu, Opt. Express **26**, 25098 (2018).
34. Y. Ye, X. Xi, C. Shi, H. Zhang, B. Yang, X. Wang, P. Zhou, and X. Xu, IEEE Photon. J. **11**, 1503508 (2019).
35. Q. Chu, Q. Shu, Z. Chen, F. Li, D. Yan, C. Guo, H. Lin, J. Wang, F. Jing, C. Tang, and R. Tao, Photon. Res. **8**, 595 (2020).
36. W. Liu, P. Ma, C. Shi, P. Zhou, and Z. Jiang, Opt. Express **26**, 15793 (2018).
37. H. Zhang, P. Zhou, H. Xiao, J. Leng, R. Tao, X. Wang, J. Xu, X. Xu, and Z. Liu, High Power Laser Sci. Eng. **6**, e51 (2018).
38. J. Dawson, M. Messerly, R. Beach, M. Shverdin, E. Stappaerts, A. Sridharan, P. Pax, J. Heebner, C. Siders, and C. Barty, Opt. Express **16**, 13240 (2008).
39. W. Zhang, Y. Rao, J. Zhu, Z. Wang, and X. Jia, Opt. Express **20**, 14400 (2012).
40. D. V. Churkin, S. A. Babin, A. E. El-Taher, P. Harper, S. I. Kablukov, V. Karalekas, J. D. Ania-Castañón, E. V. Podivilov, and S. K. Turitsyn, Phys. Rev. A **82**, 033828 (2010).
41. L. Zhang, J. Dong, and Y. Feng, IEEE J. Sel. Top. Quant. **24**, 1400106 (2018).
42. J. Dong, L. Zhang, H. Jiang, X. Yang, W. Pan, S. Cui, X. Gu, and Y. Feng, Opt. Express **26**, 5275 (2018).